

# A phosphatase complex that dephosphorylates $\gamma$ H2AX regulates DNA damage checkpoint recovery

Michael-Christopher Keogh<sup>1\*</sup>, Jung-Ae Kim<sup>4\*</sup>, Michael Downey<sup>5,7\*</sup>, Jeffrey Fillingham<sup>5,6</sup>, Dipanjan Chowdhury<sup>2,8</sup>, Jacob C. Harrison<sup>4</sup>, Megumi Onishi<sup>3</sup>, Nira Datta<sup>5,6</sup>, Sarah Galicia<sup>7</sup>, Andrew Emili<sup>5,6</sup>, Judy Lieberman<sup>2,8</sup>, Xuetong Shen<sup>9</sup>, Stephen Buratowski<sup>1</sup>, James E. Haber<sup>4</sup>, Daniel Durocher<sup>5,7</sup>, Jack F. Greenblatt<sup>5,6</sup> & Nevan J. Krogan<sup>5,6†</sup>

One of the earliest marks of a double-strand break (DSB) in eukaryotes is serine phosphorylation of the histone variant H2AX at the carboxy-terminal SQE motif to create  $\gamma$ H2AX-containing nucleosomes<sup>1</sup>. Budding-yeast histone H2A is phosphorylated in a similar manner by the checkpoint kinases Tel1 and Mec1 (ref. 2; orthologous to mammalian ATM and ATR, respectively) over a 50-kilobase region surrounding the DSB<sup>3</sup>. This modification is important for recruiting numerous DSB-recognition and repair factors to the break site, including DNA damage checkpoint proteins<sup>4,5</sup>, chromatin remodellers<sup>6</sup> and cohesins<sup>7,8</sup>. Multiple mechanisms for eliminating  $\gamma$ H2AX as DNA repair completes are possible, including removal by histone exchange followed potentially by degradation, or, alternatively, dephosphorylation. Here we describe a three-protein complex (HTP-C, for histone H2A phosphatase complex) containing the phosphatase Pph3 that regulates the phosphorylation status of  $\gamma$ H2AX *in vivo* and efficiently dephosphorylates  $\gamma$ H2AX *in vitro*.  $\gamma$ H2AX is lost from chromatin surrounding a DSB independently of the HTP-C, indicating that the phosphatase targets  $\gamma$ H2AX after its displacement from DNA. The dephosphorylation of  $\gamma$ H2AX by the HTP-C is necessary for efficient recovery from the DNA damage checkpoint.

If  $\gamma$ H2AX is dephosphorylated by a phosphoserine-specific phosphatase, it should accumulate when the relevant phosphatase is eliminated. There are about 67 phosphatases in *Saccharomyces cerevisiae*. Of the 62 not essential for cell viability, 22 are predicted to be phosphoserine protein phosphatases, and, of these, nine seem to be nuclear<sup>9</sup>. We tested the corresponding deletion strains by western analysis with the use of antibody specific for the phosphorylated form of histone H2A (Fig. 1a and Supplementary Fig. S1a). Only with deletion of *PPH3/YDR075w* did  $\gamma$ H2AX increase significantly. This phosphorylation event occurs primarily in S phase (Supplementary Fig. S2a) and is dependent on *MEC1* and *TEL1* activity (Supplementary Fig. S2b), thus probably reflecting  $\gamma$ H2AX accumulation around DSBs that occur spontaneously during DNA replication.

To characterize this putative  $\gamma$ H2AX phosphatase further, we used a strain containing a C-terminal tandem affinity purification (TAP) tag<sup>10</sup> on Pph3. After affinity purification we identified components of the highly purified protein complex by digestion with trypsin, followed by mass spectrometry<sup>11</sup>. Pph3 purified together with roughly stoichiometric amounts of two polypeptides, Ynl201c/Psy2 and Ybl046w (Fig. 1b). Tagging and purification of these two

proteins, in turn, identified the same complex: the HTP-C. Deletion of *PSY2* or *YBL046W* also increased the cellular levels of  $\gamma$ H2AX with or without DNA damage by methyl methane sulphonate (MMS) (Fig. 1c), indicating that all three proteins might work as one functional unit *in vivo*. By 4 h after removal of the MMS,  $\gamma$ H2AX levels had returned to background in wild-type cells but remained high in *pph3Δ* cells (data not shown).

To show that the HTP-C could regulate  $\gamma$ H2AX levels directly, we phosphorylated H2A *in vitro* (Supplementary Fig. S1b) and performed dephosphorylation assays with IgG-precipitated Pph3-TAP. As controls, we used immunoprecipitates of two other related and nuclear-localized, TAP-tagged phosphatases, Pph21 and Pph22 (Supplementary Fig. S1c), deletions of which have no effect on  $\gamma$ H2AX levels (Fig. 1a). Small amounts of Pph3 efficiently dephosphorylated  $\gamma$ H2AX *in vitro* (Fig. 1d), especially in the presence of  $Mn^{2+}$  rather than  $Mg^{2+}$  (Supplementary Fig. S1d), whereas much larger amounts of Pph21 or Pph22 had only marginal activity on this substrate. Therefore, *in vivo* and *in vitro* data both indicate that the HTP-C dephosphorylates  $\gamma$ H2AX. The metazoan homologue of the HTP-C is currently unclear: the PPP4c phosphatase exists in an analogous complex<sup>12</sup>, whereas the PP2A phosphatase regulates  $\gamma$ H2AX levels *in vivo*<sup>13</sup>.

To obtain further evidence that the HTP-C is related to DNA repair, we used synthetic genetic array technology<sup>14</sup> to create double mutants that were scored for growth and DNA damage sensitivity. Tetrad dissection showed that deletion of *PPH3* caused synthetic (synergistic) growth defects in combination with deletions of genes coding for homologous recombination (HR) proteins (*RAD50*, *MRE11*, *RAD51*, *RAD52* and *SAE2*), the Flap endonuclease *Rad27*, the chromatin assembly factor *Asf1*, the DNA helicase *Rrm3* and replication-fork-associated components (*TOF1*, *CSM3*, *MRC1*, *CTF8*, *CTF18* and *DCC1*) (Fig. 2a, and Supplementary Fig. S3). The fact that *pph3Δ* displayed slow-growth phenotypes when combined with deletions of DNA replication and repair genes argues that HTP-C activity is important for one or more aspects of the cellular DNA damage response. HTP-C deletions alone did not cause sensitivity to the DNA-damaging agents camptothecin, bleomycin, hydroxyurea or MMS, but double deletions such as *pph3Δ ctf18Δ* exhibited hypersensitivity to these drugs (Fig. 2b, Supplementary Fig. S3, and data not shown). We note that deletions of *PSY2* and *PPH3* were also found recently to confer sensitivity to the DNA-damaging agent cisplatin<sup>15</sup>.

<sup>1</sup>Department of Biological Chemistry and Molecular Pharmacology, <sup>2</sup>Department of Pediatrics, and <sup>3</sup>Department of Cell Biology, Harvard Medical School, Boston, Massachusetts 02115, USA. <sup>4</sup>Rosenstiel Center and Department of Biology, Brandeis University, Waltham, Massachusetts 02454, USA. <sup>5</sup>Departments of Medical Genetics and Microbiology, and <sup>6</sup>The Banting and Best Department of Medical Research, University of Toronto, Toronto, Ontario M5G 1L6, Canada. <sup>7</sup>Samuel Lunenfeld Research Institute, Mount Sinai Hospital, Toronto, Ontario M5G 1X5, Canada. <sup>8</sup>CBR Institute for Biomedical Research, Boston, Massachusetts 02115, USA. <sup>9</sup>Department of Carcinogenesis, MD Anderson Cancer Center, Smithville, Texas 78957, USA. <sup>†</sup>Present address: Department of Cellular and Molecular Pharmacology, UCSF, San Francisco, California 94143, USA.

\*These authors contributed equally to this work.

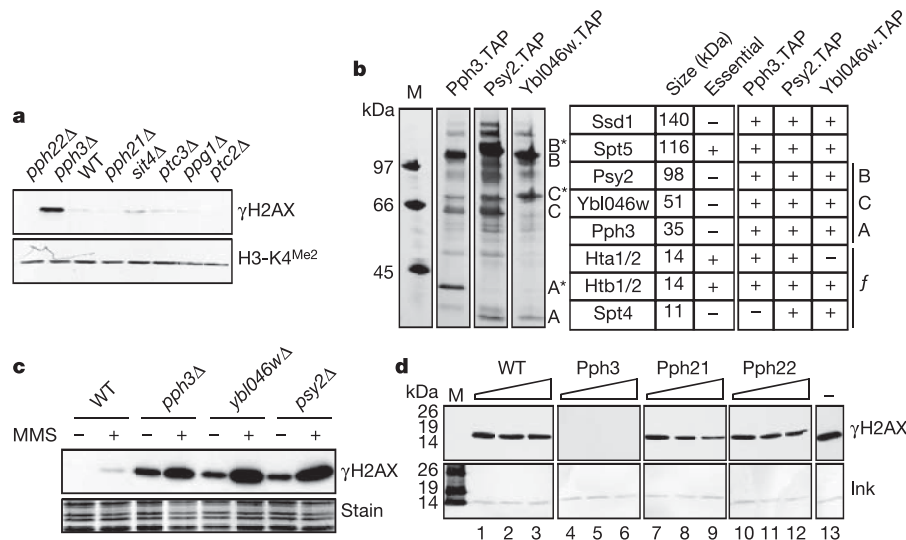


**Figure 1 | The HTP-C regulates H2A *in vivo* and dephosphorylates  $\gamma$ H2AX *in vitro*.** **a**,  $\gamma$ H2AX antibody immunoreactivity of whole cell extracts from phosphatase deletion cells (see also Supplementary Fig. S1). Lower panel, loading control. WT, wild type. **b**, Identification of Pph3-associated factors. Pph3 (A for the native protein; A\* for the calmodulin binding peptide (CBP)-tagged form) co-purified with Psy2 (B, B\*), Ybl046w (C, C\*), and substoichiometric amounts of a putative RNA exonuclease (Ssd1), Spt4/Spt5 and histones H2A (Hta1/2) and H2B (Htb1/2) (see also Supplementary Fig. S4). *f* indicates smaller proteins run off the gel and

detected by liquid chromatography/mass spectrometry. M, molecular mass marker proteins. **c**, Deletions of *PPH3*, *PSY2* or *YBL046W* increase  $\gamma$ H2AX levels in undamaged or damaged (0.05% MMS) cells. Lower panel, loading control for total protein. **d**, HTP-C is an efficient  $\gamma$ H2AX phosphatase *in vitro*. Reactions contained  $\gamma$ H2AX/H2B dimer substrate and immunoprecipitates from an untagged wild type or the indicated epitope-tagged phosphatase strains.  $\gamma$ H2AX was detected by western blotting. Lower panel, loading control for total H2A/H2B.

*S. cerevisiae* uses the homothallic (HO) endonuclease to switch mating types by creating a DSB in *MAT* and repairing the break by HR with donor sequences at *HML* or *HMR*<sup>16</sup>. Expressing HO from a galactose-inducible promoter and inserting its 24-base-pair recognition sequence at different locations provides an opportunity to monitor DSB recognition and repair<sup>17</sup>. In the experiments shown in Fig. 3a, b, HR occurred *in trans* through an uncuttable *MATa*-inc donor on chromosome V in strains lacking *HML* and *HMR* (Supplementary Table S1)<sup>18,19</sup>. HO cleavage was essentially complete within 0.5 h, repair products were detectable within 2 h, and more than 80% of cells successfully completed HR (Fig. 3a, and data not shown). After HO cleavage,  $\gamma$ H2AX appeared around the DSB and covered about 50 kilobases (kb) in less than an hour (data not shown). After about 2 h, H2A phosphorylation around the DSB began to decline (as detected by chromatin immunoprecipitation (ChIP)), with the loss at 5 kb from the DSB slightly earlier than at 10 kb, and significantly earlier than at 20 kb (Fig. 3b, and data not shown). Levels of  $\gamma$ H2AX 5 and 10 kb from the DSB declined before the final repair product appeared (detected by Southern blotting; Fig. 3a, b). Indeed, the kinetics of loss was correlated with the appearance of an early gene conversion intermediate, the beginning of new DNA synthesis from the invading 3' end of the recipient strand on the donor strand template (strand invasion-primer extension (SI-PE); Fig. 3b)<sup>20</sup>. This indicates that the signal to trigger  $\gamma$ H2AX loss might not be the completion of DSB repair but rather the completion of a step that will normally lead to repair. Note that a HR-defective *rad54* $\Delta$  strain, which fails at this SI-PE step<sup>21</sup>, has a normal  $\gamma$ H2AX-ChIP profile (Supplementary Fig. S5), again indicating that the loss of  $\gamma$ H2AX occurs after synapse formation but before the completion of repair.

DSB repair in *pph3* $\Delta$  cells was as efficient as in wild-type cells and followed the same kinetics (Fig. 3a, b). Moreover, the loss of  $\gamma$ H2AX from the DSB region in ChIP experiments occurred with rates similar to those in wild-type cells (Fig. 3a, b). Note that a high ChIP background reduced the fold increase in relative  $\gamma$ H2AX levels at the DSB in *pph3* $\Delta$  cells, possibly because the phosphorylated histone was recycled into chromatin (see below, and Supplementary Figs S6

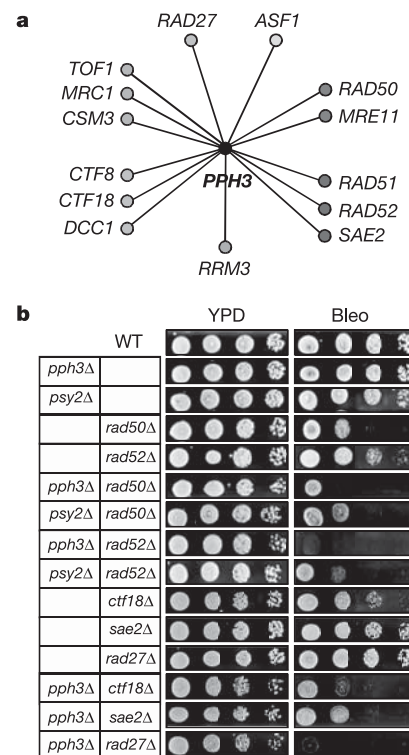


**Figure 2 | The HTP-C interacts genetically with DNA repair factors.** **a**, Lines connect genes with synthetic genetic interactions confirmed by tetrad dissection (Supplementary Fig. S3, and data not shown). **b**, Fivefold serial dilutions of various double-mutant strains on YPD plates with or without bleomycin (Bleo). WT, wild type.

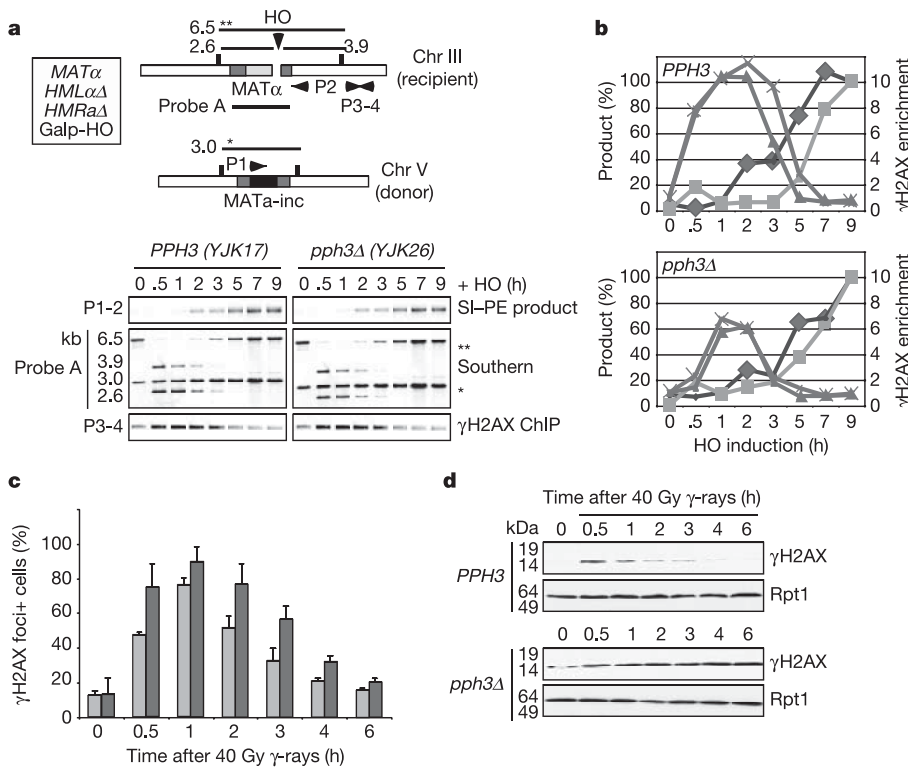


**Figure 3 | The HTP-C is not required for DSB repair and dephosphorylates displaced  $\gamma$ H2AX rather than chromatin-associated  $\gamma$ H2AX at a DSB.** **a**, Pph3 is not required for  $\gamma$ H2AX removal or efficient DSB repair by ectopic recombination. The top diagram shows the ectopic recombination system. Chr, chromosome. SI-PE (primers P1 and P2) quantifies synapse formation with donor DNA sequence. Southern blotting with probe A after digestion with *EcoRI* monitors recipient MAT $\alpha$  (uncut 6.5 kb (two asterisks), HO-cut 2.6 and 3.9 kb), donor MATa-inc (3.0 kb (asterisk), loading control) and major repair product (6.5 kb (two asterisks)). ChIP with anti- $\gamma$ H2AX 5 kb from the break site (primers P3 and P4). **b**,  $\gamma$ H2AX at a DSB disappears before completion of repair and independently of Pph3. SI-PE (diamonds) and Southern (squares) analyses in **a** are quantified relative to final repair products 9 h after HO induction. ChIP analyses are expressed as  $\gamma$ H2AX levels 5 kb (triangles) or 10 kb (crosses) from the DSB relative to an undamaged DNA region. **c**,  $\gamma$ H2AX foci disassembly after  $\gamma$ -irradiation does not require the HTP-C (200 cells counted per time point; mean and s.e.m. calculated from two independent time courses). Light grey bars, *PPH3*; dark grey bars, *pph3* $\Delta$ . **d**, Western blotting of  $\gamma$ H2AX after  $\gamma$ -irradiation in wild-type or *pph3* $\Delta$  cells. Lower panel, loading control.

and S9). We confirmed this result by staining with anti- $\gamma$ H2AX antibody to follow the kinetics of DSB repair foci after  $\gamma$ -irradiation (Fig. 3c, d).  $\gamma$ H2AX foci were efficiently disassembled by 6 h after damage in *pph3* $\Delta$  cells (Fig. 3c) even though H2A remained

phosphorylated (Fig. 3d). These results indicate that  $\gamma$ H2AX dephosphorylation might occur mainly after  $\gamma$ H2AX/H2B dimers are displaced (Supplementary Fig. S4), perhaps by a chromatin remodeller analogous to the *Drosophila* Tip60 complex<sup>22</sup>.  $\gamma$ H2AX

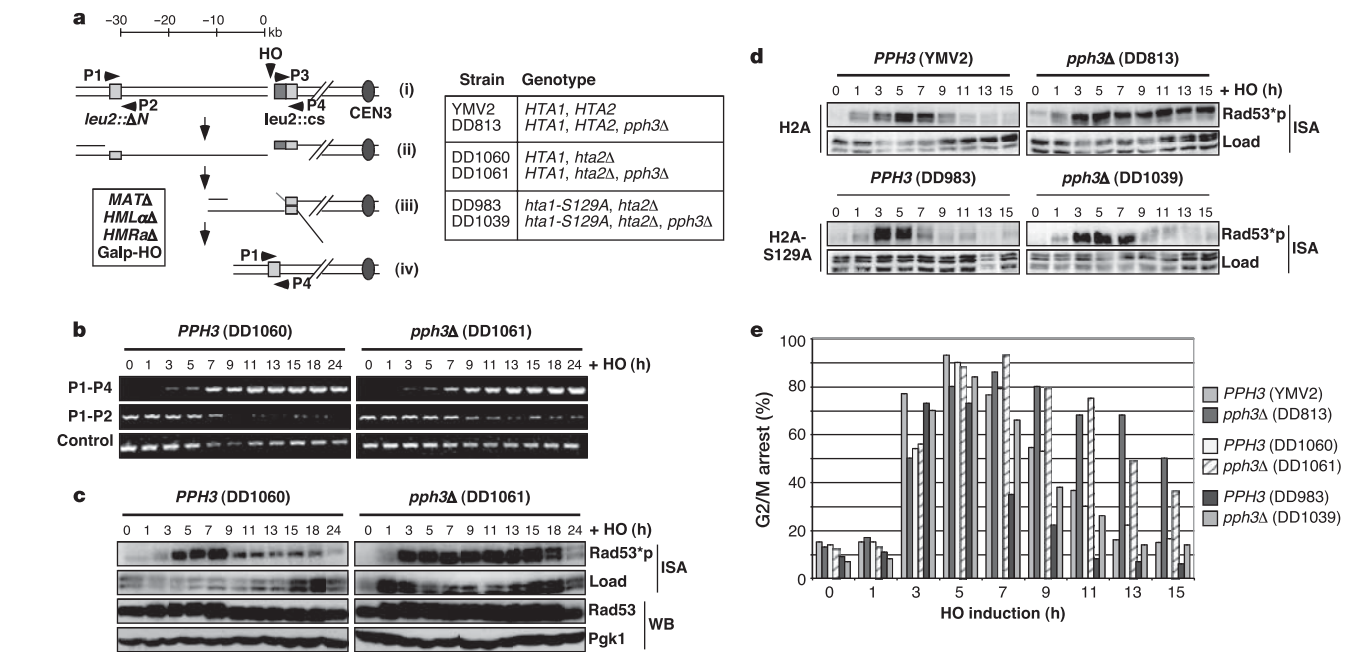


**Figure 4 |  $\gamma$ H2AX dephosphorylation by the HTP-C is required for DNA damage checkpoint recovery.** **a**, Diagram for repair by SSA of an HO-induced DSB. Top: galactose-induced HO cuts *leu2::cs*. Second row: processive 5'  $\rightarrow$  3' resection ( $4 \text{ kb h}^{-1}$ ) generates ssDNA and eventually reaches *leu2::N* $\Delta$ . Third row: the two homologous regions anneal in a Rad52- and Rad1/10-dependent fashion and the non-homologous sequences are excised. Bottom: after successful SSA the damage checkpoint is relieved<sup>19</sup>. P1–P4 are primers used for PCR analyses. Reduced histone H2A dosage has no effect on these analyses (compare YMV2 and DD1060 strains). **b**, SSA

occurs between 7 and 9 h in both wild-type and *pph3* $\Delta$  strains. This agrees with the estimated repair timing based on resection rate (8–9 h). **c**, Persistent checkpoint activation in *pph3* $\Delta$  cells monitored by Rad53 *in situ* autophosphorylation (ISA) (top panels) or mobility in western blotting (WB)<sup>30</sup>. Autophosphorylation of a non-DNA damage inducible kinase is used as a loading control. **d**, Rad53 activation does not persist in *pph3* $\Delta$  *hta1-S129A* cells. **e**, Pph3 is required for removal of the cell cycle checkpoint arrest maintained by  $\gamma$ H2AX. The graph shows the percentage of cells in G2/M arrest various times after HO induction.

is likely to be actively removed: at both 10 and 20 kb from the DSB, most of the DNA remained double-stranded after DSB repair (Supplementary Fig. S5), indicating that  $\gamma$ H2AX loss is not mediated by single-stranded DNA (ssDNA) resection.

To assess whether the DNA damage checkpoint was affected by deleting *PPH3*, we examined checkpoint activation and termination kinetics in isogenic *PPH3* and *pph3 $\Delta$*  strains with the use of the YMV2 system (Fig. 4a, and Supplementary Table S1)<sup>19</sup>. In this background *MAT*, *HML* and *HMR* are deleted, and a galactose-inducible HO cuts at an engineered site in the *LEU2* gene. The induced DSB is repaired by single-stranded annealing (SSA)<sup>23</sup> from a partial duplication of *LEU2* located 30 kb away. This repair takes about 6–7 h, during which the ssDNA formed by 5' to 3' resection triggers DNA damage checkpoint-mediated G2/M arrest and phosphorylation of the yeast checkpoint adaptor Rad9 (refs 24, 25) and Chk2 homologue checkpoint kinase, Rad53 (refs 26, 27).

*PPH3* and *pph3 $\Delta$*  cells were equally efficient in repairing the DSB (Fig. 4b), and the early kinetics of Rad53 and Rad9 activation after DSB induction was similar in both populations (Fig. 4b, top panels, and Supplementary Fig. S8c), peaking 5 h after DSB induction. However, whereas Rad53 and Rad9 activation decreased in wild-type cells 7–9 h after creation of the DSB, they remained active at least 8–9 h longer in the absence of the HTP-C (Fig. 4c, and Supplementary Fig. S8c), although these latter cells eventually recovered by 24 h. The sustained Rad53 and Rad9 activity was correlated with maintenance of the G2/M arrest (Fig. 4e). We therefore conclude that checkpoint recovery is profoundly delayed in *pph3 $\Delta$*  strains. When DNA repair is prevented, cells can escape long checkpoint-mediated G2/M arrest by adaptation<sup>28</sup>. Whereas the known recovery mutants *srs2 $\Delta$* , *ptc2 $\Delta$*  and *ptc3 $\Delta$*  are also defective in checkpoint adaptation<sup>19,29</sup>, *pph3 $\Delta$*  cells show no deficiency in the timing of the latter process (Supplementary Fig. S7).

To ascertain whether the checkpoint recovery defect of the *pph3 $\Delta$*  strain was a direct consequence of the increased  $\gamma$ H2AX levels, we mutated the H2A phosphorylation site, Ser 129, to Ala to yield *hta1-S129A* and *pph3 $\Delta$  hta1-S129A* mutant strains (Fig. 4a). Mutation of H2A Ser 129 fully restored the ability of *pph3 $\Delta$*  strains to turn off checkpoint signalling in a timely manner (Fig. 4d, bottom panels) and re-enter the cell cycle (Fig. 4e) after DNA repair. Indeed, *hta1-S129A* strains turn off checkpoint signalling (Fig. 4d) and escape G2/M arrest (Fig. 4e) slightly earlier than their wild-type counterparts. The checkpoint recovery defect imparted by the deletion of *PPH3* therefore results from the persistent phosphorylation of H2A, and it is necessary for  $\gamma$ H2AX dephosphorylation to link the DNA repair process with the termination of checkpoint signalling. One intriguing possibility is that extensive formation of  $\gamma$ H2AX for more than 50 kb around a DSB keeps the DNA damage checkpoint active until the break has been fully repaired and the modified histone has been removed from the break site and dephosphorylated by the HTP-C.

## METHODS

Full experimental details and protocols are available in the Supplementary Information. Descriptions of the yeast strains used to monitor DSB repair by ectopic recombination or single-strand annealing are found in the Supplementary Information and Supplementary Table 1. These strains employed inducible HO endonuclease to make a specific break. ChIP, Southern, SI-PE, single-strand resection, western or G2/M arrest analyses were performed in parallel as indicated.

Immunofluorescence microscopy and Western analyses were performed in parallel after DSB induction by  $\gamma$ -irradiation (40 Gy).

Double-mutant haploid strains containing both HTP-C and DNA metabolism deletions were created by synthetic genetic array technology. These double mutants were analysed for synthetic genetic interactions and sensitivity to DNA genotoxins (bleomycin, hydroxyurea or camptothecin).

*In vitro* phosphatase experiments used affinity-purified, TAP-tagged Pph3, Pph21 or Pph22 complexes. The immunopurified phosphatase was incubated with  $\gamma$ H2AX previously created *in vitro* by phosphorylating recombinant yeast

H2A/H2B dimers with RSK1. Phosphatase activity was measured by reactivity with anti- $\gamma$ H2AX antibody.

Received 19 June; accepted 1 November 2005.

Published online 20 November 2005.

- Rogakou, E. P., Pilch, D. R., Orr, A. H., Ivanova, V. S. & Bonner, W. P. DNA double-strand breaks induce H2AX phosphorylation on serine 139. *J. Biol. Chem.* **273**, 5858–5868 (1998).
- Downs, J. A., Lowndes, N. F. & Jackson, S. P. A role for *Saccharomyces cerevisiae* histone H2A in DNA repair. *Nature* **408**, 1001–1004 (2000).
- Shroff, R. et al. Distribution and dynamics of chromatin modification at a defined DNA double strand break. *Curr. Biol.* **14**, 1703–1711 (2004).
- Nakamura, T. M., Du, L. L., Redon, C. & Russell, P. Histone H2A phosphorylation controls Crb2 recruitment at DNA breaks, maintains checkpoint arrest, and influences DNA repair in fission yeast. *Mol. Cell. Biol.* **24**, 6215–6230 (2004).
- Fernandez-Capetillo, O. et al. DNA-damage induced G2-M checkpoint activation by histone H2AX and 53BP1. *Nature Cell Biol.* **4**, 993–997 (2002).
- Thiriet, C. & Hayes, J. J. Chromatin in need of a fix: phosphorylation of H2AX connects chromatin to DNA repair. *Mol. Cell* **18**, 617–622 (2005).
- Ström, L., Lindroos, H. B., Shirahige, K. & Sjögren, C. Postreplicative recruitment of cohesin to double-strand breaks is required for DNA repair. *Mol. Cell* **16**, 1003–1015 (2004).
- Ünal, E. et al. DNA damage response pathway uses histone modification to assemble a double-strand break-specific cohesin domain. *Mol. Cell* **16**, 991–1002 (2004).
- Huh, W.-K. et al. Global analysis of protein localization in budding yeast. *Nature* **425**, 686–691 (2003).
- Rigaut, G. et al. A generic protein purification method for protein complex characterisation and proteome exploration. *Nature Biotechnol.* **17**, 1030–1032 (1999).
- Krogan, N. J. et al. RNA polymerase II elongation factors of *Saccharomyces cerevisiae*: a targeted proteomics approach. *Mol. Cell. Biol.* **22**, 6979–6992 (2002).
- Gingras, A. C. et al. A novel, evolutionarily conserved protein phosphatase complex involved in cisplatin sensitivity. *Mol. Cell Proteomics* ahead of print publication, 2005 (doi:10.1074/mcp.M500231-MCP200).
- Chowdhury, D. et al.  $\gamma$ H2AX dephosphorylation by protein phosphatase 2A facilitates DNA double strand break repair. *Mol. Cell* (in the press).
- Tong, A. H. Y. et al. Systematic genetic analysis with ordered arrays of yeast deletion mutants. *Science* **294**, 2364–2368 (2001).
- Wu, H. I., Brown, J. A., Dorie, M. J., Lazzaroni, L. & Brown, J. M. Genome-wide identification of genes conferring resistance to the anticancer agents Cisplatin, Oxaliplatin and Mitomycin C. *Cancer Res.* **64**, 3940–3948 (2004).
- Haber, J. E. Mating-type gene switching in *Saccharomyces cerevisiae*. *Annu. Rev. Genet.* **32**, 561–599 (1998).
- Pâques, F. & Haber, J. E. Multiple pathways of recombination induced by double strand breaks in *Saccharomyces cerevisiae*. *Microbiol. Mol. Biol. Rev.* **63**, 349–404 (1999).
- Moore, J. K. & Haber, J. E. Cell-cycle and genetic requirements of two pathways of nonhomologous end-joining repair of double-strand breaks in *Saccharomyces cerevisiae*. *Mol. Cell. Biol.* **16**, 2164–2173 (1996).
- Vaze, M. B. et al. Recovery from checkpoint-mediated arrest after repair of a double-strand break requires Srs2 helicase. *Mol. Cell* **10**, 373–385 (2002).
- White, C. I. & Haber, J. E. Intermediates of recombination during mating type switching in *Saccharomyces cerevisiae*. *EMBO J.* **9**, 663–673 (1990).
- Sugawara, N., Wang, X. & Haber, J. E. *In vivo* roles of Rad52, Rad54 and Rad55 proteins in Rad51-mediated recombination. *Mol. Cell* **12**, 209–219 (2003).
- Kusch, T. et al. Acetylation by Tip60 is required for selective histone variant exchange at DNA lesions. *Science* **306**, 2084–2087 (2004).
- Fishman-Lobell, J., Rudin, N. & Haber, J. E. Two alternative pathways of double-strand break repair that are kinetically separable and independently modulated. *Mol. Cell. Biol.* **12**, 1292–1303 (1992).
- Lee, S. E. et al. *Saccharomyces* Ku70, Mre11/Rad50 and RPA proteins regulate adaptation to G2/M arrest after DNA damage. *Cell* **94**, 399–409 (1998).
- Vialard, J. E., Gilbert, C. S., Green, C. M. & Lowndes, N. F. The budding yeast Rad9 checkpoint protein is subjected to Mec1/Tel1-dependent hyperphosphorylation and interacts with Rad53 after DNA damage. *EMBO J.* **17**, 5679–5688 (1998).
- Matsuoka, S., Huang, M. & Elledge, S. J. Linkage of ATM to cell cycle regulation by the Chk2 protein kinase. *Science* **282**, 1893–1897 (1998).
- Blasina, A. et al. A human homologue of the checkpoint kinase Cds1 directly inhibits Cdc25 phosphatase. *Curr. Biol.* **9**, 1–10 (1999).
- Sandell, L. L. & Zakian, V. A. Loss of a yeast telomere: arrest, recovery and chromosome loss. *Cell* **75**, 729–739 (1993).
- Leroy, C. et al. PP2C phosphatases Ptc2 and Ptc3 are required for DNA checkpoint inactivation after a double-strand break. *Mol. Cell* **11**, 827–835 (2003).
- Pelliccioli, A., Lee, S. E., Lucca, C., Foiani, M. & Haber, J. E. Regulation of *Saccharomyces* Rad53 checkpoint kinase during adaptation from DNA damage-induced G2/M arrest. *Mol. Cell* **7**, 293–300 (2001).

**Supplementary Information** is linked to the online version of the paper at [www.nature.com/nature](http://www.nature.com/nature).

**Acknowledgements** We thank C. J. Ingles for critically reading the manuscript and for discussion; C. Redon, W. Hofer and N. Lowndes for antibodies; E. O'Shea and J. Weissman for yeast strains; and X. Wu, G. Zhong and X. Guo for technical assistance. N.J.K. was supported by a Doctoral Fellowship from the Canadian Institutes of Health Research (CIHR). J.C.H. and D.C. are fellows of the Leukemia and Lymphoma Society. D.D. is a recipient of the Hitchings-Elion Fellowship of the Burroughs-Wellcome Fund and a Canada Research Chair (tier II) in Proteomics, Bioinformatics and Functional Genomics. This research was supported by grants to J.F.G. from the CIHR and the Ontario Genomics Institute with funds from Genome Canada, to D.D. by the CIHR, to J.E.H. by the National Institutes of Health (NIH), and to S.B. by the NIH.

**Author Contributions** M.C.K., J.A.K. and M.D. contributed equally to this work.

N.J.K. was responsible for data in Figs 1b (with mass spectrometry help from A.E.) and 2, and Supplementary Figs 3 and 4; M.C.K. in Fig. 1d and Supplementary Fig. 1b-d (with substrate provided by M.O.), Fig. 3c (with D.C. and J.L.), d, and Supplementary Figs 6 and 9; J.A.K. in Fig. 3a, b, and Supplementary Figs 2 and 5; M.D. and D.D. in Fig. 4 and Supplementary Fig. 8a, c; J.F. in Fig. 1a; J.C.H. in Supplementary Fig. 7; S.G. in Supplementary Fig. 1a; N.D. in Supplementary Fig. 8b; and X.S. in Fig. 1c. M.C.K., S.B., J.E.H., D.D., J.F.G. and N.J.K. wrote the paper.

**Author Information** Reprints and permissions information is available at [npg.nature.com/reprintsandpermissions](http://npg.nature.com/reprintsandpermissions). The authors declare no competing financial interests. Correspondence and requests for materials should be addressed to D.D. ([durocher@mshri.on.ca](mailto:durocher@mshri.on.ca)) or J.F.G. ([jack.greenblatt@utoronto.ca](mailto:jack.greenblatt@utoronto.ca)).

## ERRATUM

doi:10.1038/nature04774

**Significant primordial star formation at redshifts  $z \approx 3-4$** 

Raul Jimenez &amp; Zoltan Haiman

*Nature* 440, 501-504 (2006)

In this Letter, the received and accepted dates were incorrect. They should read: 'Received 6 September 2005; accepted 4 January 2006.'

## CORRIGENDUM

doi:10.1038/nature04726

**Genome sequencing in microfabricated high-density picolitre reactors**

Marcel Margulies, Michael Egholm, William E. Altman, Said Attiya, Joel S. Bader, Lisa A. Bemben, Jan Berka, Michael S. Braverman, Yi-Ju Chen, Zhoutao Chen, Scott B. Dewell, Alex de Winter, James Drake, Lei Du, Joseph M. Fierro, Robin Forte, Xavier V. Gomes, Brian C. Godwin, Wen He, Scott Helgesen, Chun Heen Ho, Stephen K. Hutchison, Gerard P. Irzyk, Szilveszter C. Jando, Maria L. I. Alenquer, Thomas P. Jarvie, Kshama B. Jirage, Jong-Bum Kim, James R. Knight, Janna R. Lanza, John H. Leamon, William L. Lee, Steven M. Lefkowitz, Ming Lei, Jing Li, Kenton L. Lohman, Hong Lu, Vinod B. Makhijani, Keith E. McDade, Michael P. McKenna, Eugene W. Myers, Elizabeth Nickerson, John R. Nobile, Ramona Plant, Bernard P. Puc, Michael Reifler, Michael T. Ronan, George T. Roth, Gary J. Sarkis, Jan Fredrik Simons, John W. Simpson, Maithreyan Srinivasan, Karrie R. Tartaro, Alexander Tomasz, Kari A. Vogt, Greg A. Volkmer, Shally H. Wang, Yong Wang, Michael P. Weiner, David A. Willoughby, Pengguang Yu, Richard F. Begley & Jonathan M. Rothberg

*Nature* 437, 376-380 (2005)

In this paper, the second name of Chun Heen Ho was misspelled as He. In the earlier Corrigendum (*Nature* 439, 502; 2006) the surnames of Stephen K. Hutchison and Brian C. Godwin were misspelled as Hutchinson and Goodwin. In addition, in the Supplementary Information of the original paper, there were errors in the sequences of the DNA capture and enrichment primers, and in the formulation of emulsion oil. The Supplementary Information was updated on 4 May 2006.

## CORRIGENDUM

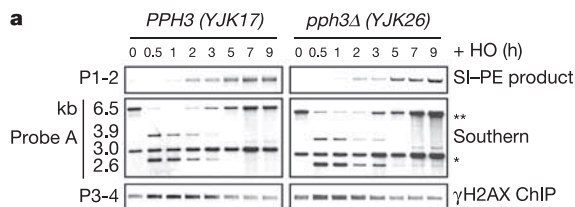
doi:10.1038/nature04772

**A phosphatase complex that dephosphorylates  $\gamma$ H2AX regulates DNA damage checkpoint recovery**

Michael-Christopher Keogh, Jung-Ae Kim, Michael Downey, Jeffrey Fillingham, Dipanjan Chowdhury, Jacob C. Harrison, Megumi Onishi, Nira Datta, Sarah Galicia, Andrew Emili, Judy Lieberman, Xueting Shen, Stephen Buratowski, James E. Haber, Daniel Durocher, Jack F. Greenblatt & Nevan J. Krogan

*Nature* 439, 497-501 (2006)

Figure 3a of this Letter contains an inadvertently duplicated panel set: those referring to '*pph3 $\Delta$*  (YJK26)' are identical to '*PPH3* (YJK17)'. The corrected panels are shown here. Note that the quantification shown in Fig. 3b refers to the correct panels. Our results and conclusions are unaffected by this oversight.



## CORRIGENDUM

doi:10.1038/nature04773

**A high-mobility electron gas at the LaAlO<sub>3</sub>/SrTiO<sub>3</sub> heterointerface**

A. Ohtomo &amp; H. Y. Hwang

*Nature* 427, 423-426 (2004)

In Fig. 2a and b of this Letter, the  $y$  axis should be labelled in units of ohms per square, not milli-ohms per square. This error does not occur elsewhere in the paper, and does not change any of our results or conclusions.